

Variation of the Gutenberg-Richter b Values and Nontrivial Temporal Correlations in a Spring-Block Model for Earthquakes

KIM CHRISTENSEN AND ZEEV OLAMI

Department of Physics, Brookhaven National Laboratory, Upton, New York

We show that a two-dimensional spring-block model for earthquakes is equivalent to a continuous, nonconservative cellular automaton model. The level of conservation is a function of the relevant elastic parameters describing the model. The model exhibits power law distributions for the energy released during an earthquake. The corresponding exponent is not universal. It is a function of the level of conservation. Thus the observed variation in the b value in the Gutenberg-Richter law could be explained by a variation in the elastic parameters. We address the problem of the boundary conditions and display results for two extreme possibilities. Furthermore, we discuss the correlation in the interoccurrence time of earthquakes. The model exhibits the features of real earthquakes: the occurrence of small earthquakes is random, while the larger earthquakes seem to be bunched. Primarily, the results of our work indicate that the dynamic of earthquakes is intimately related to the nonconservative nature of the model, which gives birth to both the change in the exponent and the correlations in interoccurrence time.

1. INTRODUCTION

In the realm of experimental physics, physicists deal with the characteristic behavior of real physical systems. In the world where theoretical physics reigns, physicists are concerned with simplified models. The majority of these models are, of course, derived from real physical systems. The golden rule, when mapping a physical system into a model system, is to grasp only the important features of the relevant phenomena. Otherwise, the model system can very easily turn out to be too complex, so that it will be almost impossible to comprehend the mechanism, which is responsible for the observed behavior.

Likewise, some insight into the complicated dynamics of earthquakes may be derived from simplistic models that contain the essential features of earthquakes. Such a simple model, a spring-block model, was proposed by *Burridge and Knopoff* [1967]. Originally, the model was defined as a two-dimensional model, but *Burridge and Knopoff* had to restrict themselves to a one-dimensional version when performing experiments and simulations. Models made up of the same basic ingredients (still in one dimension) were analyzed by several authors [*Carlson and Langer*, 1989a,b; *Nakanishi*, 1990, 1991]. A two-dimensional version of the spring-block model was simulated by *Otsuka* [1972], who also suggested a quasi-static analysis of this model. Slightly different models were later innovated by *Bak and Tang* [1989], who suggested that the idea of self-organized criticality (SOC), which was first introduced in the context of complex dynamical systems, might apply to earthquakes. Similar models were suggested by *Brown et al.* [1991], *Rundle and Brown* [1991], and *Ito and Matsuzaki* [1990]. Different models were proposed by *Feder and Feder* [1991] and *Olami et al.* [1992].

The simplest test for these models is their ability to reproduce the Gutenberg-Richter law [*Gutenberg and Richter*, 1956] which states that the rate of occurrence of earthquakes of magnitude M greater than m is given by the relation

$$\log N(M > m) = a - bm, \quad (1)$$

where a and b are constants for a given fault. Measurement of the parameter b yields a wide range of values for different faults. Values of b from 0.80 to 1.06 for small earthquakes and 1.23 to 1.54 for large earthquakes have been recorded [*Pacheco et al.*, 1992]. The energy E (proportional to the seismic moment) released during the earthquake increases exponentially with the earthquake magnitude,

$$\log E = c + dm, \quad (2)$$

where the parameter d is 1 and $\frac{3}{2}$ for small and large earthquakes, respectively [*Ekström and Dziewonski*, 1988]. By use of (1) and (2) we obtain a power law for the number of observed earthquakes with energy greater than E

$$N(E_0 > E) \sim E^{-\frac{b}{d}} = E^{-B}. \quad (3)$$

Note that B is in the same range for both small and large earthquakes, namely, 0.80 – 1.05.

While the models, simulated in the context of earthquake dynamics, produce power law for the frequency-energy distribution, they do not predict the proper B nor can they explain the variability of the B values.

Another important problem, associated with earthquake prediction, is the question of spatial and temporal correlation of earthquakes. It is observed that small earthquakes occur randomly in time. That is, the distribution of interoccurrence time of earthquakes with energy greater than E is a Poisson distribution for small E [*Johnston and Nava*, 1985]. Larger earthquakes, on the other hand, seem to be clustered [*Kagan and Jackson*, 1991]. Also, the clustered earthquakes are strongly correlated in space.

Though much effort has been addressed to correlations, especially for large earthquakes, we are not aware of any significant achievements. We believe that a more fundamental approach is required.

In this paper we map a two-dimensional version of the spring-block model for earthquakes into a continuous, non-conservative cellular automaton model. This model has several fascinating aspects. First, it exhibits a robust self-organized critical behavior over a very wide range of conservation levels. That is, we observe power law distribu-

tions for the relevant physical quantities, where the cutoff scales with the size of the system. Second, we find that the level of conservation has an impact on the power laws obtained. The level of conservation is a function of the elastic constants in the spring-block model. Therefore, the wide variances in the Gutenberg-Richter law could be interpreted as a result of the variances of the relevant elastic parameters. Finally, the model exhibits a clustering in the occurrence of large earthquakes, while the small earthquakes are distributed randomly in time.

2. THE MODEL

Burridge and Knopoff [1967] simplified the problem by discussing the internal dynamics of one single fault rather than the dynamics of a complex system of coupled faults. We consider a two-dimensional version of their model where the fault is represented by a two-dimensional network of blocks interconnected by springs. Each block is connected to the four nearest neighbors. Additionally, each block is connected to a single rigid driving plate by another set of

springs as well as connected frictionally to a fixed rigid plate (see Figure 1a). The blocks are driven by the relative movement of the two rigid plates. When the force on one of the blocks is larger than some threshold value F_{th} (the maximal static friction), the block slips. We assume that the moving block will slip to the zero force position. Slip of one block will redefine the forces on its nearest neighbors. This may lead to instabilities in the neighboring blocks and thus, as a result, in further slips and a chain reaction (earthquake) can evolve. The total number of slips following a single initial slip event is a measure of the size (seismic moment) of the earthquake

As a first step, we map the two-dimensional spring-block model into a continuous cellular automaton model. We define an $L \times L$ array of blocks by (i, j) , where i, j are integers, $1 \leq i, j \leq L$. The displacement of each block from its relaxed position on the lattice is defined as $x_{i,j}$. The total force exerted by the springs on a given block (i, j) is expressed by

$$F_{i,j} = K_1[2x_{i,j} - x_{i-1,j} - x_{i+1,j}] + K_2[2x_{i,j} - x_{i,j-1} - x_{i,j+1}] + K_L x_{i,j}, \quad (4)$$

where K_1, K_2 , and K_L denotes the elastic constants (see Figure 1b). When the two rigid plates move relative to each other, the total force on each block increases uniformly (with a rate proportional to $K_L \cdot V$, where V is the relative velocity between the two rigid plates) until one site reaches the threshold value and the process of relaxation begins (an earthquake is triggered). It can easily be shown (see Appendix A) that the redistribution of strain after a local slip at the position (i, j) is given by the relation

$$\begin{aligned} F_{i\pm 1,j} &\rightarrow F_{i\pm 1,j} + \delta F_{i\pm 1,j} \\ F_{i,j\pm 1} &\rightarrow F_{i,j\pm 1} + \delta F_{i,j\pm 1} \\ F_{i,j} &\rightarrow 0, \end{aligned} \quad (5)$$

where the increase in the force on nearest-neighbor blocks is

$$\begin{aligned} \delta F_{i\pm 1,j} &= \frac{K_1}{2K_1 + 2K_2 + K_L} \cdot F_{i,j} = \alpha_1 \cdot F_{i,j} \\ \delta F_{i,j\pm 1} &= \frac{K_2}{2K_1 + 2K_2 + K_L} \cdot F_{i,j} = \alpha_2 \cdot F_{i,j}. \end{aligned} \quad (6)$$

For simplicity, we denote the elastic ratios by α_1 and α_2 , respectively. Notice that this relaxation rule is very similar to the BTW model [Bak et al., 1987]. However, when $K_L > 0$, the redistribution of the force is nonconservative. In the context of the spring-block model, $K_L > 0$; otherwise no driving force is possible. Thus, the spring-block model is nonconservative in nature with respect to the redistribution of force. The level of conservation is $2\alpha_1 + 2\alpha_2$. However, with respect to energy (e.g., elastic energy) the model is nonconservative even if the redistribution of force is conservative. Throughout this paper the terminology "conservative" and "nonconservative" refer to the redistribution of force.

Additional differences between our new model and the old BTW model should be noticed. (1) The strain on the critical site is set to zero when relaxed. (2) The redistribution of strain to the neighbors is proportional to the strain in the relaxing site. (3) If $K_1 \neq K_2$ ($\alpha_1 \neq \alpha_2$), this model is also anisotropic. In this paper we restrict the discussion to the isotropic case $K_1 = K_2$ ($\alpha_1 = \alpha_2 = \alpha$).

The definition of the boundary conditions is a very sub-

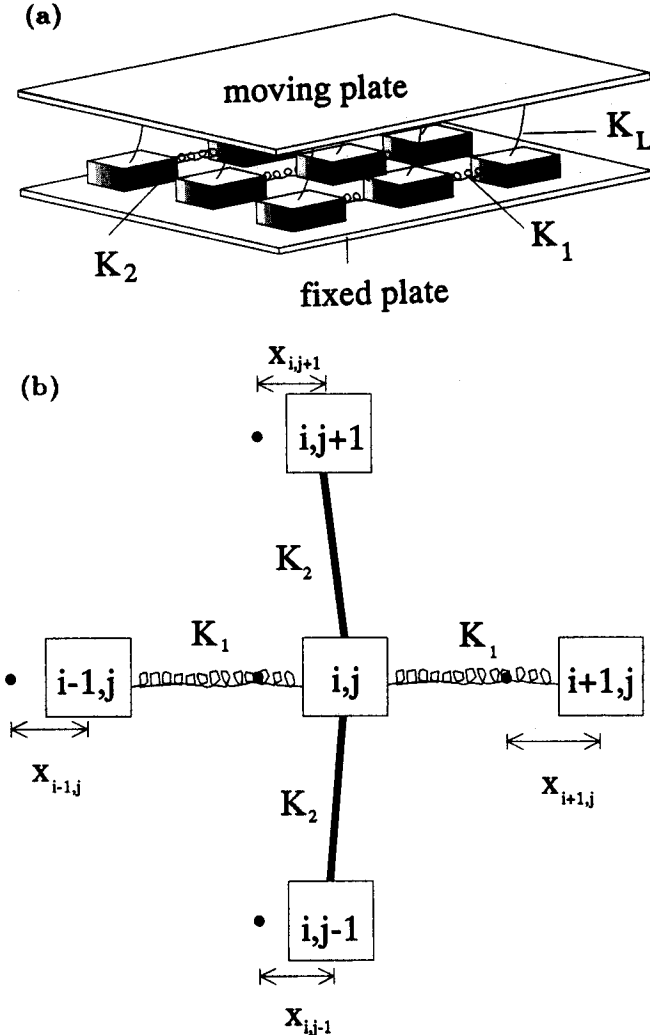


Fig. 1. The geometry of the Burridge-Knopoff spring-block model. (a) The two-dimensional system of blocks connected by springs. The strain of the blocks increases uniformly as a respond to the relative movement of the rigid plates. (b) A detailed picture of a given block (i, j) and its surroundings.

tle problem. There are two extreme possibilities: (1) The blocks in the boundary layer are connected only to blocks within the faults, the boundary is free. (2) The blocks in the boundary layer are coupled to a rigid boundary block by springs, the boundary is open. We refer to Appendix B for a detailed discussion of the boundary conditions.

Obviously, neither of the two choices is correct. It is very difficult to know what the proper boundary conditions are, and they are probably not the same for each fault. However, the actual boundary conditions must be somewhere between the two extreme limits given above. We will present results for both alternatives.

Brown *et al.* [1991] considered a model with a different geometry, $1 \leq i \leq L_x, 1 \leq j \leq L_y, L_x \gg L_y$, where L_x is the slip direction. They used free boundary conditions in the slip direction and periodic boundary conditions in the perpendicular direction. The elastic constants were chosen to fulfil the conditions $K_L \ll K_1 = K_2$. It is easy to see that this is an almost conservative model (e.g., $K_L = 1, K_1 = K_2 = 25$ imply $\alpha \approx 0.246$). In this case the free boundary conditions is almost reflective, since the effective level of conservation in the edges is 0.98. We see no physical reason to assume that $K_L \ll K_1, K_2$. A more reasonable assumption, is that all the elastic constants are in the same order of magnitude, $K_L \approx K_1 \approx K_2$. This implies that the characteristic value of α is 0.20. Rundle and Brown [1991] have investigated a square model with free boundary conditions for this particular value of α . It should be noticed that in both these models some randomness has to be introduced to avoid periodic behavior: the relaxing block does not slip to zero force position but rather to zero force position plus a random overshoot.

3. SIMULATION OF THE MODEL

The rules for the driving of our model are motivated by the dynamics of earthquakes. There are two time scales involved. One is defined by the motion of the tectonic plates, and the other is the actual duration of an earthquake. Since the first time scale is much larger than the second, we can separate the time scales. We consider the earthquake as instantaneous and do not drive the system during an avalanche. Thus the algorithm for simulating the system is the following: Define random initial strains in the system. Strain is accumulated uniformly across the system as the rigid plates move. When the strain in a certain site is above the threshold value F_{th} this site will relax according to (5) and (6). This may cause neighboring site to exceed the threshold value, in which case these sites relax simultaneously, and so on. The triggered earthquake will stop when there are no sites left with a strain above the threshold. Strain starts to accumulate once again.

We continue this process to get proper statistics of the total number of relaxations in the individual earthquakes. The total number of slips is proportional to the change in total force (which we have checked numerically) which in turn is a measure of the seismic moment (energy released). Consequently, we define the energy released during an earthquake as the total number of relaxation involved in the event.

3.1. Power Law Exponents

The continuous, nonconservative cellular automaton model exhibits SOC behavior for a wide range of α values for either boundary conditions. The exponent B depends on α and on the chosen boundary conditions. In Figure 2 we

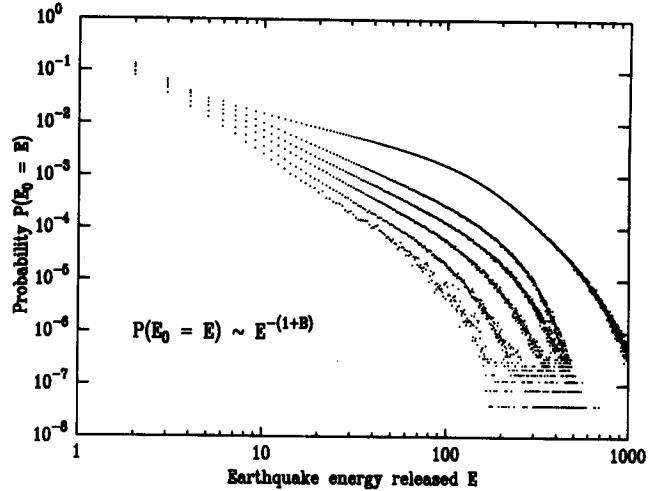


Fig. 2. Simulation results for a 35×35 system with free boundary conditions. Different curves refer to different levels of conservation. The slope of the curves become steeper as the α values is decreased. The graphs correspond to $\alpha = 0.245, 0.20, 0.15, 0.10, 0.05$ and 0.01 , respectively.

show the change of the exponent B as the level of conservation is changed for the model with free boundary conditions. In Figure 3 we display the dependence for both kinds of boundary conditions. The model has a wide range of possible exponents. For the open boundary conditions, B is between 0.22 ($\alpha = 0.25$) and 2.5 ($\alpha = 0.05$). For the free boundary conditions the range is -0.08 ($\alpha = 0.245$) to 1.35 ($\alpha = 0.01$) (notice that at exact conservation the model with free boundary conditions is not well defined because the boundary is totally reflective). The model by Rundle and Brown [1991] with free boundary conditions and $\alpha = 0.20$ gave $B = 0.6$, which is in agreement with our results.

This variability could serve as an explanation for the vari-
ances in the observed B . Note that the exponents for the

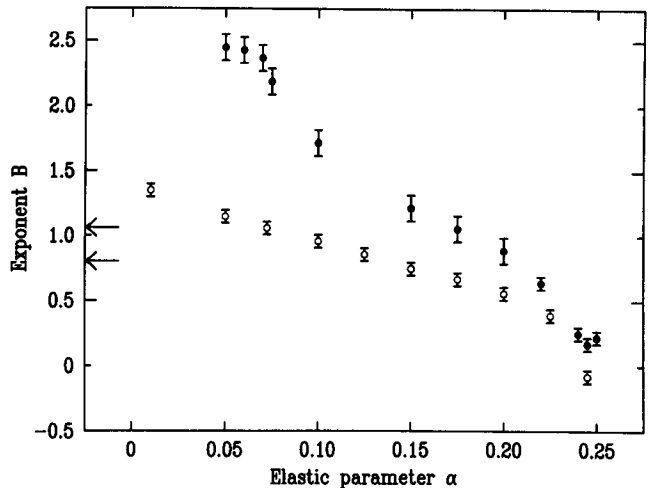


Fig. 3. The power law exponent B as a function of the elastic parameter α defined in equation (6). Solid circles correspond to the model with open boundary conditions. Below $\alpha = 0.05$ there is a transition to exponential decay. The measured B values for the model with free boundary conditions are displayed as open circles. The arrows indicate the actual measured B values for earthquakes [Pacheco *et al.*, 1992].

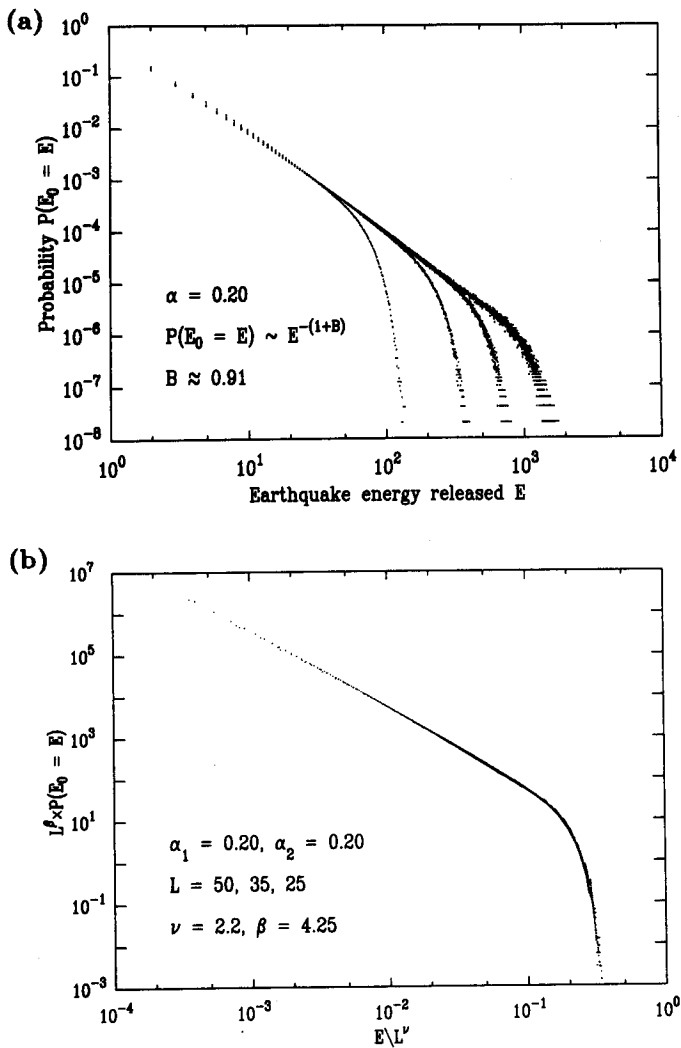


Fig. 4. (a) The probability density of having an earthquake of energy E as a function of E for $\alpha = 0.20$. The different curves refer to different system sizes $L = 15, 25, 35, 50$. (b) A finite size scaling analysis shows that the cutoff in energy distribution scales with $L^{2.2}$.

free boundary conditions are much lower than those of the open boundary conditions. This is a result of higher correlations between strains in the lattice. The relevant exponents seen for real earthquakes are near the characteristic value of $\alpha \approx 0.20$ for the open boundary conditions (see Figure 3).

We simulated the model on various lattice sizes L , using up to 5×10^7 avalanches to get accurate estimates of B . In Figure 4a we show results of simulations for the open boundary conditions with $\alpha = 0.20$ for $L = 15, 25, 35$, and 50 giving $B \approx 0.91$. By examining the scaling of the cutoff in the energy distribution as a function of the system size (*K. Christensen and Z. Olami*, manuscript submitted to *Physical Review A*, 1992) we find that the cutoff scales with $L^{2.2}$; see Figure 4b. This verifies the criticality of the model as well as the absence of any characteristic length scale associated with nonconservation. Similar results, though with different B , are obtained for the free boundary conditions.

It is clear that if $\alpha = 0$, the movement of the blocks will become completely uncorrelated due to the lack of interaction. Therefore, we expect to see a transition to a localized

behavior as α is decreased. This indeed happens for both kinds of boundary conditions but at surprisingly low α . For the open boundary conditions this occurs at $\alpha \approx 0.05$. At this value a transition between a power law behavior and exponential decay is observed. For the free boundary conditions the transition emerges in a different manner. At $\alpha \approx 0.01$ the B value is frozen and a length scale, a cutoff which is proportional to α , appears. Notice that in this case only 4% of the strain is conserved. Those transitions are obviously not relevant for earthquakes but might be related to other systems.

3.2. Spatiotemporal Clustering of Large Earthquakes

A very interesting aspect of earthquake is the correlation in the occurrence time. In Figure 5 we present two time sequences of earthquakes derived by our model, with $\alpha = 0.20$, for earthquakes with energy larger than 20 (small earthquakes) and 450 (large earthquakes), respectively. Notice that a quantitative definition of a "large earthquake" is a relative definition, since it depends on the system size. However, a qualitative definition would be that the energy released during the earthquake is so large that the event is on the edge of the power law distribution (i.e., where the distribution begins to show finite size effects).

It is evident that the two time sequences are dramatically different. The sequence for the small earthquakes seems to be distributed randomly, while for the large earthquakes it is highly clustered. The centers of clustered earthquakes in our model are generally correlated strongly in space.

The distribution function for the interoccurrence time t (the time between earthquakes) with energy greater than E , $P_E(t = t_i)$ provides a measure of those temporal correlations. Another possible measure is the coefficient of variation. It is defined as the ratio of the square root of the variance of the interoccurrence time and the average of interoccurrence time:

$$C_V(E) = \frac{\sqrt{\text{Var}_E(t)}}{\text{exp}_E(t)} \quad (7)$$

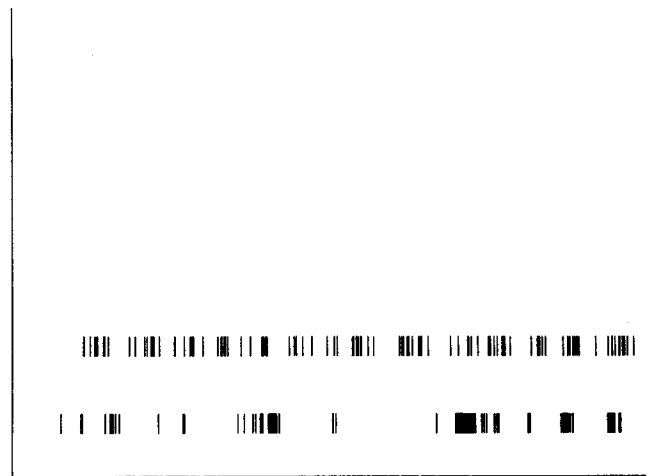


Fig. 5. A visualized sequence of earthquakes for a 35×35 system with open boundary conditions and $\alpha = 0.20$. The upper sequence shown is the occurrence of earthquakes with energy greater than or equal to 20 in a time interval of length $T = 10$. The lower sequence is the occurrence of earthquakes with energy $E \geq 450$ in a time interval of length $T \cdot \text{exp}_{450}(t) / \text{exp}_{20}(t) \approx 2410$; that is, the time intervals are scaled so that the density of points is the same.

For a random signal the distribution function is simply an exponential function yielding $C_V(E) = 1$. For a periodic signal, $C_V(E) = 0$, while clustered earthquakes will produce $C_V(E) > 1$.

We measured the coefficient of variation for the conservative model $\alpha = 0.25$ and for the characteristic value $\alpha = 0.20$ in the case of open boundary conditions. The results are presented in Figure 6.

No correlations are seen between earthquakes in the conservative model. Indeed, there seems to be some repulsion between earthquakes at intermediate energies ($C_V(E) < 1.0$). In the nonconservative model we see a clustering effects for large earthquakes, while random behavior is observed for small earthquakes. The decrease in the coefficient of variation for very large earthquakes is a finite size effect and thus is related to the cutoff in the frequency-energy distribution. Why do small earthquakes not show temporal cluster-

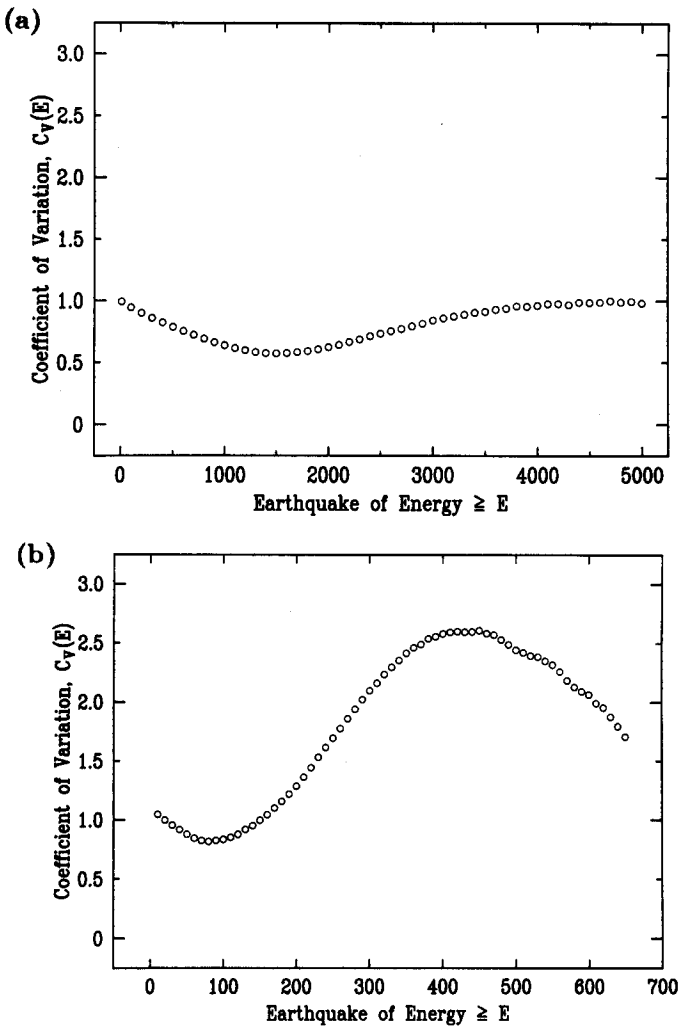


Fig. 6. The coefficient of variation $C_V(E)$ defined in equation (7) as a function of energy released during an earthquake. The results shown are for a 35×35 lattice with open boundary conditions. (a) The conservative case, $\alpha = 0.25$. Notice that $C_V(E) \leq 1$ for all E . $C_V(E) = 1$ indicates that the occurrence of earthquakes is random. (b) A nonconservative case, $\alpha = 0.20$. For small earthquakes, $C_V(E) \leq 1$. The large earthquakes are characterized by a coefficient of variation greater than 1, implying earthquake bunching.

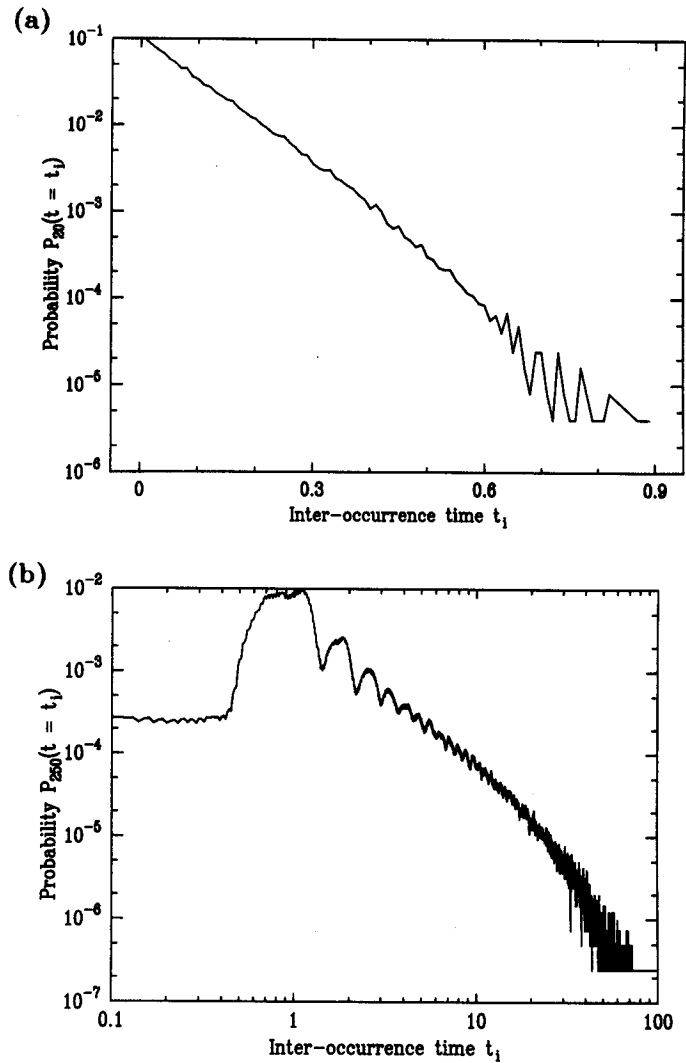


Fig. 7. The probability distribution of interoccurrence time for a 35×35 system with open boundary conditions and a level of conservation equal 0.80, $\alpha = 0.20$. (a) We consider earthquakes with energy ≥ 20 . The probability distribution is an exponential distribution. (b) Results for earthquakes with $E \geq 250$. The distribution function is a power law decaying function.

ing? The reason is that contrary to large earthquakes, small earthquakes can not be correlated in time because they are not correlated in space. They can not feel the presence of one another: a small event occurring in one part of the fault can not influence the occurrence of a small event in a totally different part of the fault. This is, of course, not true for large earthquakes.

However, if one does the same type of calculations for sub-systems (subfaults), correlations between "smaller events" (where smaller refers to the total system) will appear. This implies that it might be very useful to pay attention to the much more numerous small events to get some statistical predictions for the few large events!

We also present the distribution function for interoccurrence time for small and large earthquakes in Figures 7a and 7b respectively. We see a complete change from a random exponential distribution function to a power law decaying distribution function.

The average interoccurrence time $\exp_E(t)$ scales as E^B . However, the characteristic time between larger earthquakes within a cluster is much smaller. It is simply the buildup time for the strain in the system which is independent on E .

The time between the clusters themselves is much larger than the average interoccurrence time. Both phenomena contribute to the rise in $C_V(E)$. The average interoccurrence time between large earthquakes is a measure of the buildup time for correlations in the system.

The same kind of temporal correlations is seen in real earthquakes. Small earthquakes seem to be uncorrelated; see Figure 6 of *Johnston and Nava* [1985]. Large earthquakes display strong clustering; see *Kagan and Jackson* [1991]. It might be very interesting to make the same kind of calculation for an earthquake catalog of some fault.

These results are closely related to the fact that the model is nonconservative. The occurrence of large earthquakes in such a model is related to creation of correlated strains in the fault. Otherwise, the earthquakes would become completely localized. Since the correlations are not completely destroyed by intermediate shocks, clustering will occur with correlated centers. The nonconservative nature of the model creates correlations in the strain of a fault, which is an important feature in the creation of the relevant power laws and temporal correlation. The earthquakes are generated by correlated clusters of sites, which in turn are generated by the earthquakes themselves. The correlated sites are modified by interactions with other clusters through earthquakes.

For conservative models, however, large earthquakes involve a lot of activity inside the fault which completely destroy any correlations existing in the lattice. This explains why the earthquakes in a conservative model can not be correlated in time.

4. CONCLUSION

The results presented in this paper indicate very strongly that earthquakes are related to nonconservative SOC models. The nonconservative nature of the model is induced through the relaxation rules. The effects of this dissipative nature are quite profound. It creates a variation of the exponents and the existence of nontrivial temporal correlations in the system. Both features seem to be in accord with what is observed for actual earthquakes. This introduces a new set of ideas which appears to be associated with the problem of earthquake temporal and spatial correlations. We believe that further theoretical and experimental effort can clarify those intriguing problems.

As to the generality of the model we can only speculate. We believe that most nonconservative models which display criticality, i.e., power law behavior where the cutoffs scale with system size, are, at least qualitatively, similar to the model presented in this paper. The strong argument for this is that in order to create power law distribution functions in a nonconservative model, the model must be able to correlate in space. This will lead to temporal correlations as we have demonstrated in this model.

We may be able to improve our ability to estimate the probabilities of occurrence of large earthquakes, even with the limited information available about the history of earthquake occurrence and existing faults by utilizing the information hidden in the numerous small events!

APPENDIX A

Assume that the strain of a block at position (i, j) is above the threshold value, that is,

$$F_{th} \leq F_{i,j} = K_1 \cdot [2x_{i,j} - x_{i-1,j} - x_{i+1,j}] + K_2 \cdot [2x_{i,j} - x_{i,j-1} - x_{i,j+1}] + K_L \cdot x_{i,j}. \quad (8)$$

If $\tilde{x}_{i,j}$ denotes the displacement of block (i, j) from the relaxed position after the block has slipped to zero force position, then

$$0 = K_1 \cdot [2\tilde{x}_{i,j} - x_{i-1,j} - x_{i+1,j}] + K_2 \cdot [2\tilde{x}_{i,j} - x_{i,j-1} - x_{i,j+1}] + K_L \cdot \tilde{x}_{i,j}, \quad (9)$$

where we exploits the fact that nearest-neighbor blocks can not be supercritical at the same time, why

$$x_{i\pm 1,j} = \tilde{x}_{i\pm 1,j} \\ x_{i,j\pm 1} = \tilde{x}_{i,j\pm 1}. \quad (10)$$

The slipping block (i, j) affects the strain on the nearest-neighbor blocks. As an example, we calculate the change of force on block $(i, j+1)$. The force on block $(i, j+1)$ is

$$F_{i,j+1} = K_1 \cdot [2x_{i,j+1} - x_{i-1,j+1} - x_{i+1,j+1}] + K_2 \cdot [2x_{i,j+1} - x_{i,j} - x_{i,j+2}] + K_L \cdot x_{i,j+1}. \quad (11)$$

Thus the change of force due to a slip a position (i, j) is

$$\delta F_{i,j+1} = -K_2 \cdot dx_{i,j}. \quad (12)$$

Notice that the force on block $(i, j+1)$ may very well be affected by a slip at position $(i, j+2)$ but that does not interfere this argument. An expression for the change in displacement of block (i, j) ,

$$dx_{i,j} = \tilde{x}_{i,j} - x_{i,j} \quad (13)$$

is obtained by subtracting (8) from (9):

$$0 - F_{i,j} = [2K_1 + 2K_2 + K_L] \cdot dx_{i,j}. \quad (14)$$

Finally, substituting (14) into (12), we find

$$\delta F_{i,j+1} = \frac{K_2}{2K_1 + 2K_2 + K_L} \cdot F_{i,j}. \quad (15)$$

APPENDIX B

The boundary condition is free if the blocks in the boundary layer are connected only to blocks within the fault; that is, the force on a boundary block, say at site (i, L) , is given by

$$F_{i,L} = K_1 \cdot [2x_{i,j} - x_{i-1,j} - x_{i+1,j}] + K_2 \cdot [x_{i,j} - x_{i,j-1}] + K_L \cdot x_{i,j}. \quad (16)$$

If this block slips, we find

$$0 - F_{i,L} = [2K_1 + K_2 + K_L] \cdot dx_{i,L}, \quad (17)$$

resulting in

$$\delta F_{i\pm 1,L} = \frac{K_1}{2K_1 + K_2 + K_L} \cdot F_{i,L} = \alpha_{bc} \cdot F_{i,L}. \quad (18)$$

If the model is isotropic, $K_1 = K_2 = K$, then

$$\alpha = \frac{K}{4 \cdot K + K_L}. \quad (19)$$

We can express the elastic ratio α_{bc} used when boundary blocks slips in terms of α

$$\alpha_{bc} = \frac{\alpha}{1 - \alpha}. \quad (20)$$

If a block in one of the corners slips, we use

$$\tilde{\alpha}_{bc} = \frac{\alpha}{1 - 2 \cdot \alpha}. \quad (21)$$

For a simulation of the model with open boundary conditions we use the same α all over the lattice. That is, if block (i, L) slips we still increase the force on the three neighboring blocks ($i \neq 1, L$) with an amount equal to $\alpha \cdot F_{i,L}$, where α is defined in (6).

Acknowledgments. We would like to thank Per Bak for introducing us to this subject. K. Christensen gratefully acknowledge the financial support of Carlsbergfondet, Augustinus Fonden, Løvens Kemiske Fabriks Forskningsfond, and the Danish Research Academy. Z. Olami thanks the Weizmann and Fullbright Foundations for support during this research. Both authors appreciate the support and hospitality of Brookhaven National Laboratory. This work was supported by the Division of Basic Energy Sciences, U.S.DOE under contract DE-AC02-76CH00016.

REFERENCES

- Bak, P., and C. Tang, Earthquakes as a self-organized critical phenomenon, *J. Geophys. Res.*, **94**, 15635-15637, 1989.
- Bak, P., C. Tang, and K. Wiesenfeld, Self-organized criticality: An explanation of $1/f$ noise, *Phys. Rev. Lett.*, **59**, 381-384, 1987.
- Brown, S. R., C. H. Scholz, and J. B. Rundle, A simplified spring-block model of earthquakes, *Geophys. Res. Lett.*, **18**, 215-218, 1991.
- Burridge, R., and L. Knopoff, Model and theoretical seismicity, *Bull. Seismol. Soc. Am.*, **57**, 341-371, 1967.
- Carlson, J. M., and J. S. Langer, Properties of earthquakes generated by fault dynamics, *Phys. Rev. Lett.*, **62**, 2632-2635, 1989a.
- Carlson, J. M., and J. S. Langer, A mechanical model of an earthquake fault, *Phys. Rev. A*, **40**, 6470-6484, 1989b.
- Ekström, G., and A. M. Dziewonski, Evidence of bias in estimations of earthquake size, *Nature*, **332**, 319-323, 1988.
- Feder, H. J. S., and J. Feder, Self-organized criticality in a stick-slip process, *Phys. Rev. Lett.*, **66**, 2669-2672, 1991.
- Gutenberg, B., and C. F. Richter, Magnitude and energy of earthquakes, *Ann. Geofis.*, **9**, 1, 1956.
- Ito, K., and M. Matsuzaki, Earthquakes as a self-organized critical phenomena, *J. Geophys. Res.*, **95**, 6853-6860, 1990.
- Johnston, A. C., and S. J. Nava, Recurrence rates and probability estimates for the New Madrid seismic zone, *J. Geophys. Res.*, **90**, 6737-6753, 1985.
- Kagan, Y. Y., and D. D. Jackson, Long-term earthquake clustering, *Geophys. J. Int.*, **104**, 117-133, 1991.
- Nakanishi, H., Cellular-automaton model of earthquakes with deterministic dynamics, *Phys. Rev. A*, **41**, 7086-7089, 1990.
- Nakanishi, H., Statistical properties of the cellular-automaton model for earthquakes, *Phys. Rev. A*, **43**, 6613-6621, 1991.
- Olami, Z., H. J. S. Feder, and K. Christensen, Self-organized criticality in a continuous, nonconservative cellular automaton modeling earthquakes, *Phys. Rev. Lett.*, **68**, 1244-1247, 1992.
- Otsuka, M., A simulation of earthquake occurrence, *Phys. Earth Planet. Inter.*, **6**, 311-315, 1972.
- Pacheco, J. F., C. H. Scholz, and L. R. Sykes, Changes in frequency-size relationship from small to large earthquakes, *Nature*, **355**, 71-73, 1992.
- Rundle, J. B., and S. R. Brown, Origin of rate dependence in frictional sliding, *J. Stat. Phys.*, **65**, 403-412, 1991.
- K. Christensen and Z. Olami, Department of Physics, Brookhaven National Laboratory, Bldg. 510A, Upton, NY 11973.

(Received October 3, 1991;
revised January 13, 1992;
accepted January 30, 1992.)